



## CHAPTER V

### SOLUTION PROPERTIES AND VESICLE FORMATION OF RHAMNOLIPID BIOSURFACTANTS PRODUCED BY *Pseudomonas aeruginosa* SP4

#### 5.1 Abstract

A biosurfactant produced by *Pseudomonas aeruginosa* strain SP4 was previously reported as a mixture of eleven types of rhamnolipid compounds. Among them, the major component in the biosurfactant was characterized as L-rhamnosyl-3-hydroxydecanoyl-3-hydroxydecanoate, or mono-rhamnolipid (Rha-C<sub>10</sub>-C<sub>10</sub>). In this present study, solution properties of the biosurfactant were investigated in a phosphate-buffer saline (PBS) solution (pH 7.4) by using surface tension, turbidity, electrical conductivity, and dynamic light scattering (DLS) measurements. It was found that spherical biosurfactant vesicles of various sizes (ranging from 50 to larger than 250 nm) were spontaneously formed at a biosurfactant concentration greater than its critical micelle concentration (CMC), which was 200 mg/l. The encapsulation efficiency (*E*%) of the biosurfactant vesicles was preliminarily studied by using Sudan III, a water-insoluble dye, as a model hydrophobic substance. The obtained results showed that the vesicle formed in the PBS solution at a biosurfactant concentration of 1280 mg/l could entrap about 10% of the initial hydrophobic dye concentration. The effects of salt and alcohol on the vesicle formation of the biosurfactant and its encapsulation efficiency were also observed using sodium chloride (NaCl) and ethanol (C<sub>2</sub>H<sub>5</sub>OH), respectively. In the presence of either NaCl or C<sub>2</sub>H<sub>5</sub>OH, the vesicle size was reduced from larger than 250 nm to 50–250 nm. The encapsulation efficiency of the biosurfactant vesicle was slightly influenced by the addition of NaCl, but was significantly increased, up to nearly 30%, in the presence of C<sub>2</sub>H<sub>5</sub>OH.

**Keywords:** Biosurfactants; Glycolipids; Rhamnolipids; *Pseudomonas aeruginosa*; Solution properties; Vesicle formation

## 5.2 Introduction

*Pseudomonas aeruginosa* strains, Gram-negative bacteria, have been reported to excrete a mixture of biosurfactants with a glycolipid structure. These are known as rhamnolipids. Although there are many types of rhamnolipids, all of them possess similar chemical structures [1]. Generally, rhamnolipids contain a hydrophilic head formed by one or two rhamnose molecules and a hydrophobic tail composed of one or two fatty acid chains [2], as shown in Figure 5.1. The two major types of rhamnolipids are L-rhamnosyl-3-hydroxydecanoyl-3-hydroxydecanoate, or monorhamnolipid (Rha-C<sub>10</sub>-C<sub>10</sub>), and L-rhamnosyl-L-rhamnosyl-3-hydroxydecanoyl-3-hydroxydecanoate, or dirhamnolipid (Rha-Rha-C<sub>10</sub>-C<sub>10</sub>). However, most of the biosurfactants produced by *P. aeruginosa* strains have been reported to be dirhamnolipid [3-7]; only a few reports have shown that monorhamnolipid was the predominant component [8,9]. The difference in type and proportion of rhamnolipid compounds in the excreted biosurfactant has been proposed to be governed by the age of the culture, the selected bacterial strain [10], substrate composition, and specific culture conditions [11].

From the point of view of surfactant properties, rhamnolipids are one of the most interesting biosurfactants [12]. Rhamnolipids can reduce the surface tension of pure water from 72 to below 30 mN/m with a critical micelle concentration (CMC) in the range of 5–200 mg/l, depending on the rhamnolipid components in the excreted biosurfactant [13]. Rhamnolipids are able to maintain their surface activities even under extreme conditions of temperature and pH [14]. In addition, rhamnolipids also possess distinguishing biological activities, including anti-proliferative activity against a human breast cancer cell line (MCF-7) [15], and anti-microbial activity against both bacteria and phytopathogenic fungi species [16,17]. Recently, dirhamnolipid, which is a major type of rhamnolipid, has been reported to promote the wound healing process because of its effect on keratinocytes and fibroblasts [18].

Like other synthetic surfactants, biosurfactants are able to form a variety of microstructures such as spherical, globular, and cylindrical micelles; spherical and

irregular vesicles; tubular and irregular bilayers; lamellar sheets; and, lyotropic liquid crystalline phases with lamellar, hexagonal, and cubic symmetries [19]. The morphology of these surfactant aggregates are affected by surfactant concentration [2], pH [20], temperature [21], counterions [22], ionic strength [23], and cosolutes or contaminants like alcohols and metals [20,24]. In the case of rhamnolipids, it has been demonstrated that the aggregate structures of a monorhamnolipid can be affected by pH, cadmium, and octadecane [20], while those of a dirhamnolipid are affected by biosurfactant concentration [2]. One of the most important functions of these molecular aggregates is the solubilization capacity. The mechanism and technique of solubilization are used in many products, such as cleaning products, pharmaceuticals, cosmetics, and food [25,26]. However, the solubilization capacity of rhamnolipid aggregates has rarely been studied. Further knowledge about the aggregation behavior of rhamnolipid biosurfactants could perhaps be used to introduce these surface-active molecules into high value-added applications in the near future, enlarging their potential applications.

The *P. aeruginosa* strain SP4 is able to produce a biosurfactant when grown in a nutrient broth supplemented with palm oil as a carbon source. After being fractionated by using a high performance liquid chromatograph (HPLC) equipped with an evaporative light scattering detector (ELSD), six high-purity rhamnolipid-containing fractions were obtained. With the use of Fourier transform infrared (FT-IR) spectroscopy in combination with  $^1\text{H}$  nuclear magnetic resonance ( $^1\text{H}$  NMR) analysis, and mass spectrometry, the chemical structure of the most relatively abundant fraction was identified as Rha-C<sub>10</sub>-C<sub>10</sub>, while the structures of the remaining fractions were characterized as Rha-Rha-C<sub>8</sub>-C<sub>10</sub>, Rha-C<sub>8</sub>-C<sub>10</sub>, Rha-C<sub>10</sub>-C<sub>12</sub>, Rha-C<sub>10</sub>-C<sub>12</sub>, and Rha-Rha-C<sub>10</sub>-C<sub>14.1</sub>, with small contributions from their structural isomers [14]. In this present study, the solution properties of the biosurfactant produced by *P. aeruginosa* strain SP4 were investigated in a phosphate-buffer saline (PBS) solution (pH 7.4). Spontaneous vesicle formation was observed, and its encapsulation efficiency was evaluated by using Sudan III, a water-insoluble dye, as a model hydrophobic substance, in order to study the potential use of the rhamnolipid vesicle in either delivery systems or other dispersed

systems. The effects of additives like salt and alcohol on the vesicle formation and its encapsulation efficiency were also investigated by using sodium chloride (NaCl) and ethanol (C<sub>2</sub>H<sub>5</sub>OH), respectively.

### 5.3 Experimental

#### 5.3.1 Materials

Both sodium chloride (NaCl) (99.0% purity) and ethanol (C<sub>2</sub>H<sub>5</sub>OH) (99.8% purity) were purchased from Labscan Asia Co., Ltd. (Thailand). 1-[4-(phenylazo)phenylazo]-2-naphthol, or Sudan III, (90% dye content) was supplied by Sigma. (The chemical structure of the Sudan III is shown in Figure 5.2.) All chemicals were used as received without further purification.

#### 5.3.2 Production and Chemical Structures of Rhamnolipid Biosurfactants

*P. aeruginosa* strain SP4, a biosurfactant-producing microorganism, was isolated from petroleum-contaminated soil in Thailand [27]. The isolated strain was maintained on nutrient agar slants at 37°C and was sub-cultured every 2 weeks. To produce the biosurfactant, an inoculum was first prepared by transferring the bacterial colonies into a nutrient broth, and the culture was incubated at 37°C in a shaking incubator at 200 rpm for 22 h. Then a nutrient broth containing 2% inoculum and 2% palm oil was incubated at 37°C under aerobic conditions in a shaking incubator at 200 rpm for 48 h to obtain the highest microbial and biosurfactant concentrations [27]. After that, the culture medium was centrifuged at 4°C and 8500 rpm for 20 min to remove the bacterial cells. The obtained supernatant was further treated by acidification to pH 2.0 using 6 M hydrochloric acid solution, and the acidified supernatant was left overnight at 4°C for complete precipitation of the biosurfactant [28]. After centrifugation, the precipitate was removed and was dissolved in a 0.1 M sodium bicarbonate solution, followed by the biosurfactant extraction step with a solvent having a 2:1 chloroform-to-ethanol ratio at room temperature [29]. The organic phase was transferred to a round-

bottom flask connected to a rotary evaporator in order to remove the solvent. After solvent evaporation, about 5.20 g of a viscous honey-colored biosurfactant product was extracted per liter of the culture medium. The chemical structure of the most abundant component in the biosurfactant product was identified as Rha-C<sub>10</sub>-C<sub>10</sub> (73.48%), while the others were characterized as Rha-Rha-C<sub>8</sub>-C<sub>10</sub> (0.68%), Rha-C<sub>8</sub>-C<sub>10</sub> (1.54%), Rha-C<sub>10</sub>-C<sub>12.1</sub> (9.55%), Rha-C<sub>10</sub>-C<sub>12</sub> (13.35%), and Rha-Rha-C<sub>10</sub>-C<sub>14.1</sub> (1.39%) with small contributions of their structural isomers [14].

### 5.3.3 Preparation of Rhamnolipid Biosurfactant Solution

The aqueous solution of the extracted biosurfactant was prepared by using a direct dissolution method. A specific amount of the extracted biosurfactant was simply dissolved in the PBS solution (pH 7.4) either in the absence or presence of the additive (NaCl or C<sub>2</sub>H<sub>5</sub>OH) to any desired concentration. To achieve a homogeneous solution, the sample was vortexed at room temperature, and was then filtered through a 0.45- $\mu$ m pore size nylon filter at least two times in order to remove any dust. All of the measurements were performed one day after sample preparation, and no measurement was done on a prepared solution which exhibited two separate macroscopic phases.

### 5.3.4 Analytical Methods and Measurements

#### 5.3.4.1 *Surface Tension Measurement*

The surface tension of the PBS solution either in the absence or presence of the additives at different biosurfactant concentrations were measured by a drop shape analysis system (Krüss, DSA10 Mk2). The surface tension measurements were carried out at room temperature (25–27°C) by using the pendant drop method. All of the measurements were repeated three times and their average values were used. The critical micelle concentration (CMC) was then determined from the break point of surface tension *versus* its log of bulk concentration curve. For the calibration of the instrument, the surface tension of pure water was measured before each set of experiments.

#### 5.3.4.2 *Turbidity Measurement*

The turbidity of the prepared biosurfactant solutions was measured by using a UV/Vis spectrophotometer (Shimadzu, UV-2550) at room temperature. The reported values were corresponded to the absorbance at a wavelength ( $\lambda$ ) equal to 600 nm [2].

#### 5.3.4.3 *Electrical Conductivity Measurement*

It is known that the change in the electrical conductivity of a surfactant-containing solution relates to the aggregation of the surfactant molecules [30,31], so the electrical conductivity of the biosurfactant solution was determined using a dynamic light scattering instrument (Brookhaven, ZetaPALS) at  $25\pm 1^\circ\text{C}$ .

#### 5.3.4.4 *Dynamic Light Scattering Measurement*

The dynamic light scattering (DLS) technique was employed to measure the sizes of the biosurfactant vesicles formed at various conditions. The same dynamic light scattering instrument (Brookhaven, ZetaPALS) was used at  $90^\circ$  scattering angle and  $25\pm 1^\circ\text{C}$ . The sizes of the biosurfactant vesicles were calculated from the diffusion coefficients obtained from computer analysis using the software provided with the instrument.

#### 5.3.4.5 *Transmission Electron Microscopy Examination*

The morphology of the biosurfactant vesicles was observed with transmission electron microscopy (TEM) by using the negative-staining technique. A drop of the test biosurfactant solution sample was placed onto a copper grid, and was stained with 1% uranyl acetate aqueous solution. The excess of the biosurfactant solution was removed by adsorbing the drop with a piece of filter paper. The grid was dried in a vacuum desiccator for at least 6 h. The samples were imaged under a transmission electron microscope (JEOL, JEM-2100).

#### 5.3.5 Encapsulation Experiment

The encapsulation efficiency of the biosurfactant vesicles was evaluated by using Sudan III, a water-insoluble dye, as a model hydrophobic compound. A stock

solution of Sudan III was first prepared in chloroform at a concentration of 1.23 mg/ml. Then, 100  $\mu$ l of the stock solution was added to an empty vial, and the solvent was evaporated in a vacuum oven until dry. After that, 10 ml of the biosurfactant solution at a concentration of 1280 mg/l was added into the vial, and was allowed to equilibrate for 1 week. The residual insoluble dye was separated from the mixture by centrifugation at 10,000 rpm for 10 min. The color supernatant was further filtered through a 0.45- $\mu$ m pore size nylon filter at least two times, and the amount of the entrapped dye was determined from the absorbance at a wavelength of 512 nm using the UV/Vis spectrophotometer. The concentration of the entrapped dye was calculated by using a calibration curve of Sudan III prepared in chloroform in the concentration range of 0.10 to 12.30 mg/l. The encapsulation efficiency ( $E\%$ ) was defined as the ratio of the concentration of the entrapped Sudan III to the initial dye concentration.

#### 5.3.6 Statistical Analysis

The experimental data are presented in terms of arithmetic averages of at least three replicates, and the standard deviations are indicated by the error bars. The analyses were done using SigmaPlot software, version 8.02 (SPSS Inc., UK).

### 5.4 Results and Discussion

#### 5.4.1 Surface Activity and Solution Properties

Because of a difficulty in the separation of the rhamnolipid components into a single homologue, the individual contribution of each rhamnolipid homologue to the biosurfactant product has not been elucidated, and the whole biosurfactant solution as a mixed biosurfactant system was investigated instead. The biosurfactant produced by *Pseudomonas* species is always characterized as a single surface-active compound with special properties [32]. While the surface-active properties of the biosurfactant produced by *P. aeruginosa* strains are affected by the ratio and composition of the rhamnolipid species, those of each rhamnolipid homologue can be impacted by the presence of

unsaturated bonds, the length of alkyl chains, and the size of the hydrophilic head group [33]. For example, it has been reported that dirhamnolipid (Rha-Rha-C<sub>10</sub>-C<sub>10</sub>) showed a CMC of about 5 mg/l, while the CMC of monorhamnolipid (Rha-C<sub>10</sub>-C<sub>10</sub>) was found to be 40 mg/l [34]. More hydrophilic homologues, both Rha-Rha-C<sub>10</sub> and Rha-C<sub>10</sub>, displayed CMCs of 200 mg/l [4]. The CMCs of rhamnolipids containing unsaturated hydrophobic chains were found to be greater than those of the corresponding saturated forms [35], and it was also suggested that the presence of larger fatty acid chains decreased the CMCs of the rhamnolipid species [3].

In this present study, the surface activity of the biosurfactant produced by *P. aeruginosa* SP4, which has previously been identified as a mixture of 11 types of rhamnolipid species, was studied by using surface tension measurement. Figure 5.3a shows the plot of surface tension *versus* biosurfactant concentration. It was found that the surface tension of the PBS solution (pH 7.4) was rapidly reduced as the biosurfactant concentration increased. However, a decrease in the surface tension was not quite uniform due to the presence of two transition points in the plot, which is different from the usual surfactant systems. The first shape drop was at the biosurfactant concentration of 40 mg/l, while the second one was at the biosurfactant concentration of about 200 mg/l. Cohen and Exerowa [36] measured the surface tension of aqueous solutions of mixtures of mono- and dirhamnolipids, and reported a step-like surface tension reduction. In that study, there were three transition zones in the plot of the surface tension *versus* the concentration of the rhamnolipid mixture. The first shape drop was assumed to relate to an aggregation and pre-micelle formation of rhamnolipid molecules, while the second one corresponded to the micelle formation of the monorhamnolipid in the solution. The third one was determined to be the CMC of the rhamnolipid mixture, because the surface tension remained unchanged beyond this point. In some mixed surfactant systems, it is possible that surfactant molecules with a difference in hydrophobicity aggregate and form respective micelles at different concentrations, leading to the presence of more than one transition point in the surface tension curve [32, 36]. In the present study, the first transition point, at the biosurfactant concentration



of 40 mg/l, is believed to relate to the micelle formation of mono-rhamnolipid, which was previously characterized as a major component in the extracted biosurfactant [14]. This value (40 mg/l) was also very much accordant with the reported CMC of monorhamnolipid [33]. The second transition point, at the biosurfactant concentration of 200 mg/l, is considered to be the CMC of the extracted biosurfactant, because the surface tension remained constant beyond this biosurfactant concentration with a minimum surface tension of about 29 mN/m.

To further study the aggregation of rhamnolipid molecules in the biosurfactant produced by *P. aeruginosa* strain SP4, turbidity measurements were first carried out. Figure 5.4a shows the turbidity of the biosurfactant solution prepared in PBS solution as a function of the biosurfactant concentration. When the biosurfactant concentration was very low (less than 200 mg/l), the solution turbidity increased with increasing biosurfactant concentration. Beyond a biosurfactant concentration of 200 mg/l (the CMC), the solution turbidity sharply increased with increasing biosurfactant concentration. Normally, a change in the turbidity of a surfactant solution relates to the change in the amount or size of the surfactant aggregates. Therefore, the obtained results can imply either an increase in the amount or the size of the biosurfactant aggregates in the PBS solution with increasing biosurfactant concentration.

It is known that the electrical conductivity of a surfactant solution can be used to indicate the structure of surfactant aggregates, so electrical conductivity measurements were subsequently done. Figure 5.5a shows the relationship between the solution conductivity and the biosurfactant concentration. The solution conductivity abruptly increased with increasing biosurfactant concentration. Interestingly, the maximum solution conductivity was found at a biosurfactant concentration of 80 mg/l, implying new information about a change in the aggregate structure of the rhamnolipid molecules at this biosurfactant concentration (which will be further discussed later). The solution conductivity started decreasing at a biosurfactant concentration higher than 80 mg/l, and finally remained constant when the biosurfactant concentration was greater than 600 mg/l. Kakizawa *et al.* [37] studied the solution properties of double-tailed

cationic surfactants having ferrocenyl groups in their hydrophobic moieties. They reported that a decrease in the electrical conductivity of a surfactant solution corresponded to the vesicle formation. When the vesicular structure formed, the ions in the inner aqueous phase were separated by the alkyl chains of the bilayer membrane. Therefore, the electric charge is reduced, and the solution conductivity decreases. Zhai *et al.* [38] also reported that the change in the solution conductivity in this manner could be interpreted as the formation of closed bilayer structures. Based on those two previous works, the vesicular structure of rhamnolipid biosurfactants is hypothesized to form at a biosurfactant concentration greater than 80 mg/l, and the biosurfactant vesicles should be the predominant structure at a biosurfactant concentration greater than 200 mg/l (the CMC).

Dynamic light scattering measurement was also performed in order to investigate the aggregation of the biosurfactant in more detail, because the light intensity scattered from the surfactant solution can be used to indicate the aggregation and the change in the size of the surfactant aggregates [37]. In the present study, the scattered light intensity is expressed as an average light scattering count rate. Figure 5.6a shows the relationship between the average count rate and the biosurfactant concentration in the absence of additives. The average count rate remained constant at low biosurfactant concentrations (less than 10 mg/l), and then rapidly increased when the biosurfactant concentration increased to above 40 mg/l. The sharp increase in the average count rate implies the aggregation of the rhamnolipid molecules. The average count rate began to level off when the biosurfactant concentration further increased above 80 mg/l. From the results, it can be concluded that monorhamnolipid molecules, the major component in the extracted biosurfactant, first aggregate into the micellar structure at a biosurfactant concentration of 40 mg/l. Then the rhamnolipid vesicles gradually form in the biosurfactant concentration range of 80 to 200 mg/l, and spontaneous vesicle formation is finally observed when the biosurfactant concentration is greater than 200 mg/l, which is determined to be the CMC of the studied biosurfactant (see Figure 5.3a).

To obtain an overall picture of the aggregation behavior of the biosurfactant, the dynamic light scattering measurement was also employed to determine the aggregate size (hydrodynamic diameter). The results showed that small aggregates with an average size of approximately 10 nm, which were most likely micellar structures of monorhamnolipid [20], formed at a biosurfactant concentration greater than 40 mg/l. These small aggregates gradually disappeared, and the heterogeneous sizes of the aggregates were observed in the biosurfactant concentration range of 80 to 200 mg/l. When the biosurfactant concentration was greater than 200 mg/l, a bimodal distribution of aggregate sizes was observed: 50–250 and >250 nm. Based on the work of Champion *et al.* [20], the aggregates with sizes in the 50 to 250 nm range are classified as a medium vesicular structure, while those larger than 250 nm are considered to be a large vesicular structure. As shown in Figure 5.7a, these two vesicular structures coexisted when the biosurfactant concentration was increased to about 1200 mg/l. A further increase in the biosurfactant concentration beyond 1200 mg/l resulted in the disappearance of the medium-size vesicles.

To verify the presence of the above-mentioned biosurfactant vesicles, transmission electron microscopy (TEM) was used to observe the morphology of the biosurfactant vesicles. Although the negative-staining technique might affect the size of the biosurfactant vesicles, it was found to be very much in accord with the data obtained from the dynamic light scattering measurement. Figures 5.8a and 5.8b show the representative negative-staining electron micrographs of the biosurfactant vesicles formed in the PBS solution at two different biosurfactant concentrations. From the TEM micrographs, an increase in the biosurfactant concentration from 320 to 2560 mg/l significantly increased the size of the biosurfactant vesicles. The TEM micrograph at the biosurfactant concentration of 320 mg/l showed mainly medium spherical vesicles (50–250 nm), while that at the biosurfactant concentration of 2560 mg/l was found to have only the large spherical vesicles (> 250 nm). It has been reported that rhamnolipid biosurfactants can form the lamella structure in a concentrated solution [2,20,39]. However, the highest biosurfactant concentration of 2560 mg/l used in this study is not

high enough to obtain the lamella structure. In addition, it is known that pH is another important factor affecting the structures of surfactant aggregates. In the case of rhamnolipids, Champion *et al.* investigated the effect of pH on the aggregate structure of monorhamnolipid, and they reported that the lamella structures were not observed when the pH of the rhamnolipid solution was higher than 7.0 [20]. This was explained in that rhamnolipids undergo changes in the diameter of the hydrophilic head group, depending on the protonation state of the carboxyl group. An increase in the solution pH can increase the negative charge of the hydrophilic moiety of rhamnolipid, so the repulsion force between the adjacent hydrophilic head groups of rhamnolipids increases, leading to a larger head diameter. Hence, the formation of a large aggregate structure like the lamellar structure was disfavored. In the present study, the aggregate structure of the rhamnolipid biosurfactant was investigated at pH 7.4; therefore, the effect of pH perhaps explains why the lamella structures did not appear in the studied biosurfactant concentration range.

#### 5.4.2 Effect of Salt

To study the effect of salt on the solution properties and vesicle formation of the biosurfactant produced by *P. aeruginosa* SP4, NaCl, which was frequently used in dispersed systems, was added to the biosurfactant solution, and the NaCl concentration was varied at 0.1, 0.2, and 0.4 M. Figure 5.3b shows the plot of surface tension *versus* biosurfactant concentration in the presence of NaCl at three different concentrations. It was observed that the two-transition point phenomenon still existed, regardless of the variation in the NaCl concentration. The CMC and the minimum surface tension also remained unchanged, suggesting a good level of tolerance to ionic strength of the extracted biosurfactant.

The turbidity measurement was also performed after the addition of NaCl to the biosurfactant solutions. As shown in Figure 5.4b, the turbidity of the biosurfactant solution in the presence of NaCl is lower than that in the absence of NaCl, and it decreases with an increase in the NaCl concentration for any given biosurfactant

concentration. The decrease in the solution turbidity by added NaCl implies that the size of the biosurfactant aggregates should be reduced after the addition of NaCl.

The effect of NaCl on the electrical conductivity of the biosurfactant solution is shown in Figure 5.5b. For any given NaCl concentration, the solution conductivity first increased with an increase in the biosurfactant concentration, and reached a maximum at a biosurfactant concentration of 80 mg/l. Beyond 80 mg/l, the solution conductivity decreased with increasing biosurfactant concentration, and then leveled off at a biosurfactant concentration greater than 1200 mg/l. A similar trend of the obtained results suggests that the addition of NaCl does not significantly affect the micelle formation of monorhamnolipid and the formation of the biosurfactant vesicle. However, the solution conductivity was found to significantly increase with increasing NaCl concentration. Kakizawa *et al.* [37] reported that the electrical conductivity of the surfactant solution increased when the vesicle became smaller. Therefore, the electrical conductivity results indicate a reduction of the aggregate size by the addition of NaCl. An increase in the solution conductivity also implies an increase in the dispersion stability of the small-sized biosurfactant aggregates as well.

Figure 5.6b shows the effect of NaCl on the average light scattering count rate of the biosurfactant solutions having different biosurfactant concentrations. For any given NaCl concentration, the average count rate first remained constant at low biosurfactant concentrations, and then rapidly increased at a biosurfactant concentration above 40 mg/l. The average count rate began to decrease at a biosurfactant concentration greater than 80 mg/l. Thus, the biosurfactant concentration at which the change in the average count rate occurred agreed well with that obtained from the electrical conductivity measurement. From the dynamic light scattering measurement, the aggregate size was gradually reduced with an increase in the NaCl concentration, and the medium vesicular structure finally coexists with the large one even at a biosurfactant concentration greater than 1200 mg/l when the NaCl concentration increases to 0.4 M, as shown in Figure 5.7b. Figure 5.8c is a TEM micrograph of the biosurfactant vesicles formed at a biosurfactant concentration of 2560 mg/l in a PBS solution containing 0.4 M

NaCl. Comparing this to the TEM micrograph of the biosurfactant vesicles formed in the PBS solution, Figure 5.5a, it can be seen that the predominant morphology in the presence of 0.4 M NaCl is the medium spherical vesicles.

The addition of electrolytes to the solution of ionic surfactants generally resulted in the screening effect on the electrostatic repulsion between the charged aggregates, so the energy required for the transfer of the surfactant ions from the bulk solution to the aggregates is decreased [40]. The addition of the electrolyte promotes the aggregation of ionic surfactants, and the growth of the aggregates can be affected by the solubility of the surfactants in the media. Nyuta *et al.* [41] reported that the presence of NaCl could increase the water solubility of a heterogemini surfactant, and that the sizes of the aggregates were reduced after the addition of NaCl. For rhamnolipid biosurfactants, our results are also supported by the work of Helvacı *et al.*, who reported that the aggregate sizes of both mono- and dirhamnolipids were significantly reduced when the NaCl concentration was increased [39].

Rhamnolipid compounds are composed of carboxylic groups in their chemical structures (Figure 5.1). When the pH is above 4.0, the majority of these carboxylic groups are dissociated to form carboxylate groups, and rhamnolipids begin to behave as anions or soft bases [33]. In the presence of NaCl, sodium ions ( $\text{Na}^+$ ) in the solution act as a soft acid, so they can easily bind with the carboxylate groups in the chemical structures of the rhamnolipids, resulting in the induction of the solvated groups. When the concentration of NaCl increases, the amount of solvated groups increases, thereby improving the water solubility of the biosurfactant. In addition, the counterion exchange to  $\text{Na}^+$  at the non-dissociated carboxylic groups also affected the water solubility of the biosurfactant. Although the added NaCl promotes the aggregation of the ionic surfactants, an increase in the water solubility of the biosurfactant molecules perhaps disfavors the growth of the aggregates. Hence, the size of the biosurfactant vesicles was found to be reduced after the addition of NaCl.

#### 5.4.3 Effect of Alcohol

To study the effect of alcohol on the solution properties and on the vesicle formation of the biosurfactant produced by *P. aeruginosa* strain SP4, C<sub>2</sub>H<sub>5</sub>OH, which is frequently used in the formulation of emulsions, was added to the biosurfactant solution; the C<sub>2</sub>H<sub>5</sub>OH concentration was varied at 0.1, 0.2, and 0.4 M. Figure 5.3c shows the plot of surface tension *versus* biosurfactant concentration at various C<sub>2</sub>H<sub>5</sub>OH concentrations. Interestingly, the two transition points were also found to exist in the plot, but the biosurfactant concentrations at the transition points were different from those in the absence of C<sub>2</sub>H<sub>5</sub>OH. At a C<sub>2</sub>H<sub>5</sub>OH concentration of 0.1 or 0.2 M, the first transition point was observed at a biosurfactant concentration of 40 mg/l. As the C<sub>2</sub>H<sub>5</sub>OH concentration increased to 0.4 M, it shifted from 40 to 80 mg/l. The second transition point, the CMC, increased from 200 mg/l in the absence of C<sub>2</sub>H<sub>5</sub>OH to nearly 300 mg/l after the addition of C<sub>2</sub>H<sub>5</sub>OH at a concentration of 0.1 M. As the C<sub>2</sub>H<sub>5</sub>OH concentration increased to either 0.2 or 0.4 M, the second transition point further increased to about 600 mg/l. Therefore, the addition of C<sub>2</sub>H<sub>5</sub>OH into the biosurfactant solutions seems to disfavor the aggregation of rhamnolipid molecules. As shown in Figure 5.4c, the turbidity of the biosurfactant solution in the presence of C<sub>2</sub>H<sub>5</sub>OH is lower than that in the absence of C<sub>2</sub>H<sub>5</sub>OH, and it further decreases with an increase in the C<sub>2</sub>H<sub>5</sub>OH concentration. From the turbidity results, it was confirmed that the size of the biosurfactant aggregate was reduced after the addition of the C<sub>2</sub>H<sub>5</sub>OH.

Figure 5.5c illustrates the relationship between the solution conductivity and the biosurfactant concentration at three different C<sub>2</sub>H<sub>5</sub>OH concentrations. At a C<sub>2</sub>H<sub>5</sub>OH concentration of 0.1 M, it was found that the solution conductivity first increased with an increase in the biosurfactant concentration, but the slope of the line gradually changed at a biosurfactant concentration of 40 mg/l. The solution conductivity reached a maximum value at a biosurfactant concentration of 80 mg/l, and began to decrease with a further increase in the biosurfactant concentration. At a C<sub>2</sub>H<sub>5</sub>OH concentration of 0.2 M, although the biosurfactant concentration at which the slope of the line changed was still the same as that at the C<sub>2</sub>H<sub>5</sub>OH concentration of 0.1 M, the

biosurfactant concentration at which the solution conductivity began to decrease shifted from 80 to 160 mg/l. As the  $C_2H_5OH$  concentration was increased to 0.4 M, the biosurfactant concentration at which the slope of the line changed increased from 40 to 80 mg/l, while the biosurfactant concentration at which the solution conductivity began to reduce was 160 mg/l. Generally, it was observed that the solution conductivity increased with an increase in the  $C_2H_5OH$  concentration, indicating a reduction of the vesicle size in the presence of  $C_2H_5OH$ . Therefore, the results suggest that the addition of  $C_2H_5OH$  to the biosurfactant solution significantly affects the aggregation of rhamnolipid molecules.

The influence of added  $C_2H_5OH$  on the average light scattering count rate is shown in Figure 5.6c. For a  $C_2H_5OH$  concentration of 0.1 M, the average count rate first remained unchanged at low biosurfactant concentrations, and then rapidly increased with increasing biosurfactant concentration. The average count rate reached a maximum value at a biosurfactant concentration of 80 mg/l, and began to decrease when the biosurfactant concentration further increased. For any further increase in  $C_2H_5OH$  concentration to 0.2 or 0.4 M, the profile of the average count rate appeared similar, except it shifted to higher biosurfactant concentrations, and the maximum value of the average count rate was also found to be higher. The biosurfactant concentration at which the change in the average count rate occurred also agreed with that obtained from the electrical conductivity measurement.

The dynamic light scattering results show that the contribution of a medium vesicular structure increased with increasing  $C_2H_5OH$  concentration. As shown in Figure 5.7c, only the medium vesicular structure exists at the  $C_2H_5OH$  concentration of 0.4 M. Figure 5.8d is the TEM micrograph of the biosurfactant vesicles formed at a biosurfactant concentration of 2560 mg/l in the PBS solution with 0.4 M  $C_2H_5OH$ . Compared to the TEM micrograph of the biosurfactant vesicles formed in the PBS solution without additives, Figure 5.8a, the predominant morphology in the presence of 0.4 M  $C_2H_5OH$  was medium spherical vesicles.



Since rhamnolipid compounds are soluble in  $C_2H_5OH$ , the presence of  $C_2H_5OH$  in the investigated system can improve the solubility of the studied biosurfactant. As a result, the presence of  $C_2H_5OH$  disfavors rhamnolipid aggregation, and the CMC increases. The effect of  $C_2H_5OH$  on the size of the biosurfactant vesicles is expected to be governed by the interactions in the outer bilayer region [35]. The added  $C_2H_5OH$  is composed of hydrophilic and hydrophobic parts in its chemical structure, so it acts as a co-surfactant and interacts with the rhamnolipid molecules via the hydrogen bond forming between the hydroxyl group of the  $C_2H_5OH$  and those in the hydrophilic head group (rhamnose moiety) of the rhamnolipid molecule, leading to the formation of rhamnolipid- $C_2H_5OH$  mixed vesicles. The presence of  $C_2H_5OH$  in the aggregate membrane increases the surface area at which the charge is localized, resulting in a reduction of the surface charge density. Hence, the dissociation of rhamnolipid molecules increases, and the electrostatic repulsion between the polar head groups of the surfactant molecules in the aggregates increases, thereby disfavoring the growth of the surfactant aggregates and finally reducing the aggregate size.

#### 5.4.4 Encapsulation Results

The formation of surfactant vesicles has received much attention in recent years because the vesicles can encapsulate either water-soluble (in their inner aqueous phase) or oil-soluble substances (in their outer bilayer region), resulting in the potential use as a vehicle, or carrier, for effective compounds in drug, gene, and transdermal delivery [42]. In the present study, the biosurfactant produced by *P. aeruginosa* SP4 could spontaneously form the vesicular structure upon increasing the biosurfactant concentration. Thus, the ability of the biosurfactant vesicles to encapsulate the desired substances was subsequently investigated to observe the potential use of the biosurfactant vesicles in delivery systems. Sudan III, a water-insoluble dye, was used as a model hydrophobic substance in order to evaluate the encapsulation efficiency ( $E\%$ ) of the biosurfactant vesicles. The effects of salt and alcohol on the encapsulation efficiency were studied at different NaCl and  $C_2H_5OH$  concentrations for applications in

physiological solutions and for the incorporation of alcohol in the vesicle formulation, respectively. To ensure the spontaneous vesicle formation, the encapsulation experiment was done at a high biosurfactant concentration of 1280 mg/l (several times the CMC).

The encapsulation efficiency of the biosurfactant vesicles formed at different additive concentrations is shown in Figure 5.9. In the absence of the additives, the biosurfactant vesicle could entrap only about 10% of the initial Sudan III dye concentration (0.96 mg of entrapped Sudan III per gram of biosurfactant). By the addition of NaCl, the encapsulation efficiency of the biosurfactant vesicles slightly decreased with an increase in the NaCl concentration. When the NaCl concentration increased to 0.4 M, the encapsulation efficiency was reduced to 6% (0.58 mg/g). A decrease in vesicle size with increasing NaCl concentration lowers the encapsulation efficiency. In contrast, the addition of C<sub>2</sub>H<sub>5</sub>OH significantly increased the encapsulation efficiency of the biosurfactant vesicles. It was found that the biosurfactant vesicles could entrap around 30% of the hydrophobic dye (3.26 mg/g) when the concentration of C<sub>2</sub>H<sub>5</sub>OH increased to 0.4 M. An increase in the encapsulation efficiency after the addition of C<sub>2</sub>H<sub>5</sub>OH might be caused by the formation of a rhamnolipid-C<sub>2</sub>H<sub>5</sub>OH mixed vesicle, because the incorporation of C<sub>2</sub>H<sub>5</sub>OH in the vesicle membrane increased the solubilization of the hydrophobic dye in the outer bilayer region. The controlling ability of the biosurfactant vesicles to entrap the desired substance in the presence of the additives suggests the potential use of rhamnolipids in delivery systems. In addition, it was reported that rhamnolipids were very compatible with skin as compared to a synthetic surfactant [43]. Therefore, rhamnolipid vesicles can perhaps meet the criteria for entrapping active ingredients in skin care products.

## 5.5 Conclusions

In this present study, the solution properties of the biosurfactant produced by *P. aeruginosa* SP4 were investigated in a PBS solution (pH 7.4). The spontaneous formation of rhamnolipid vesicles with various sizes was observed at a biosurfactant

concentration greater than its critical micelle concentration (200 mg/l). By the addition of an additive, either NaCl or C<sub>2</sub>H<sub>5</sub>OH, to the biosurfactant solution, the higher the additive concentration, the smaller the size of the biosurfactant vesicle. The ability of the biosurfactant vesicles to entrap Sudan III, a model hydrophobic substance, both in the absence and presence of the additives suggests the potential use of the rhamnolipid vesicles in delivery systems.

## 5.6 Acknowledgements

This work was financially supported by The Thailand Research Fund (TRF) under an RGJ Ph.D. scholarship and an BRG 5080030 Grant, and The Research Unit of Applied Surfactants for Separation and Pollution Control, supported by Chulalongkorn University. The authors also thank Meditop Co., Ltd (Thailand) for providing the Brookhaven ZetaPALS instrument used in both electrical conductivity and dynamic light scattering measurements.

## 5.7 References

- [1] J.L. Torrens, D.C. Herman, R.M. Miller-Maier, *Environmental Science and Technology*, 32 (1998) 776.
- [2] M. Sánchez, F.J. Aranda, M.J. Espuny, A. Marqués, J.A. Teruel, Á. Manresa, A. Ortiz, *Journal of Colloid and Interface Science*, 307 (2007) 246.
- [3] J.C. Mata-Sandoval, J. Karns, A. Torrent, *Microbiological Research*, 155 (2001) 249.
- [4] K.S.M. Rahman, T.J. Rahman, S. McClean, R. Marchant, I.M. Banat, *Biotechnology Progress*, 18 (2002) 1277.
- [5] E. Haba, A. Pinazo, M.J. Espuny, M.R. Infante, A. Manresa, *Biotechnology and Bioengineering*, 81 (2003) 316.

- [6] A. Perfumo, I.M. Banat, F. Canganella, R. Marchant, *Applied Microbiology and Biotechnology*, 72 (2006) 132.
- [7] S.A. Monteiro, G.L. Sasaki, L.M. de Souza, J.A. Meira, J.M. de Araújo, D.A. Mitchell, L.P. Ramos, N. Krieger, *Chemistry and Physics of Lipids*, 147 (2007) 1.
- [8] S. Arino, R. Marchal, J.P. Vandecasteele, *Applied and Environmental Microbiology*, 45 (1996) 162.
- [9] L. Sim, O.P. Ward, Z.Y. Li, *Journal of Industrial Microbiology and Biotechnology*, 19 (1997), 232.
- [10] E. Déziel, F. Lépine, D. Dennie, D. Boismenu, O.A. Mamer, R. Villemur, *Biochimica et Biophysica Acta*, 1440 (1999) 244.
- [11] S.G.V.A.O. Costa, M. Nitschke, R. Haddad, M.N. Eberlin, J. Contiero, *Process Biochemistry*, 41 (2006) 483.
- [12] S.S. Cameotra, R.S., Makkar, *Current Opinion in Microbiology*, 7 (2004) 262.
- [13] W.R. Finnerty, *Environmental Biotechnology*, 5 (1994) 291.
- [14] O. Pornsunthorntawe, P. Wongpanit, S. Chavadej, M. Abe, R. Rujiravanit, *Bioresource Technology*, 99 (2008) 1589.
- [15] B. Thanomsub, W. Pumeechockchai, A. Limtrakul, P. Arunrattiyakorn, W. Petchleelaha, T. Nitoda, *Bioresource Technology*, 97 (2006) 2457.
- [16] A. Abalos, A. Pinazo, M.R. Infante, M. Casals, F. García, A. Manresa, *Langmuir*, 17 (2001) 1367.
- [17] M. Benincasa, A. Abalos, I. Oliveira, A. Manresa, *Antonio van Leeuwenhoek*, 85 (2004) 1.
- [18] T. Stipcevic, T. Piljac, R.R. Isseroff, *Journal of Dermatological Science*, 40 (2005) 141.
- [19] P.K. Vinson, Y. Talmon, A. Walter, *Biophysical Journal*, 56 (1989) 669.
- [20] J.T. Champion, J.C. Gilkey, H. Lamparski, J. Reitner, R.M. Miller, *Journal of Colloid and Interface Science*, 170 (1995) 569.
- [21] M. S. Bakshi, S. Sachar, *Journal of Colloid and Interface Science*, 296 (2006) 309.

- [22] N. Jiang, P. Li, Y. Wang, J. Wang, H. Yan, R. K. Thomas, *Journal of Colloid and Interface Science*, 286 (2005) 755.
- [23] J. Mata, T. Joshi, D. Varade, G. Ghosh, P. Bahadur, *Colloids and Surfaces A: Physicochemical and Engineering Aspects*, 247 (2004) 1.
- [24] M. Villeneuve, N. Ikeda, K. Motomura, M. Artono, *Journal of Colloid and Interface Science*, 208 (1998) 388.
- [25] A. Saeki, H. Sakai, K. Kamogawa, Y. Kondo, N. Yoshino, H. Uchiyama, J. H. Harwell, M. Abe, *Langmuir*, 2000 (16) 9991.
- [26] M. Abe, A. Saeki, K. Kamogawa, H. Sakai, Y. Kondo, N. Yoshino, H. Uchiyama, J. H. Harwell, *Industrial and Engineering Chemistry Research*, 2000 (39) 2697.
- [27] O. Pornsunthorntawe, N. Arttaweeporn, S. Paisanjit, P. Somboonthanate, M. Abe, R. Rujiravanit, S. Chavadej, *Biochemical Engineering Journal*, 42 (2008) 172.
- [28] M.M. Yakimov, H.L. Fredrickson, K.N. Timmis, *Biotechnology Applied Biochemical*, 23 (1996) 13.
- [29] Y. Zhang, R.M. Miller, *Applied and Environmental Microbiology*, 58 (1992) 3276.
- [30] R. Zana, B. Michels, *Langmuir*, 14 (1998) 6599.
- [31] Y. Fan, M. Cao, G. Yuan, Y. Wang, H. Yan, C. C. Han, *Journal of Colloid and Interface Science*, 299 (2006) 928.
- [32] R. Cohen, D. Exerowa, *Advances in Colloid and Interface Science*, 134 (2007) 24.
- [33] M. Nitschke, S.G.V.A.O. Costa, J. Contiero, *Biotechnology Progress*, 21 (2005) 1593.
- [34] S. Lang, F. Wagner, *Biosurfactants and Biotechnology*, Marcel Dekker, New York, 1987.
- [35] E. Haba, A. Abalos, O. Jauregui, M.J. Espuny, A. Manresa, *Journal of Surfactants and Detergents*, 6 (2003) 155.
- [36] F. Han, X. He, J. Huang, Z. Li, Y. Wang, H. Fu, *Journal of Physical Chemistry B*, 108 (2004) 5256.
- [37] Y. Kakizawa, H. Sakai, K. Nishiyama, M. Abe, *Langmuir*, 12 (1996) 921.

- [38] L. Zhai, X. Tan, T. Li, Y. Chen, X. Huang, *Colloids and Surfaces A: Physicochemical and Engineering Aspects*, 276 (2006) 28.
- [39] Ş. Ş. Helvacı, S. Peker, G. Özdemir, *Colloids and Surfaces B: Biointerfaces*, 35 (2004) 225.
- [40] D. Attwood, A. Terreros, E. Lopez-Cabarcos, P.A. Galera-Gomez, *Journal of Colloid and Interface Science*, 225 (2000) 25.
- [41] K. Nyuta, T. Yoshimura, K. Esumi, *Journal of Colloid and Interface Science*, 301 (2006) 267.
- [42] W. Worakitkanchanakul, T. Imura, T. Fukuoka, T. Morita, H. Sakai, M. Abe, R. Rujiravanit, S. Chavadej, H. Minamikawa, D. Kitamoto, *Colloids and Surfaces B: Biointerfaces*, 65 (2008) 106.
- [43] G. Özdemir, Ö.E. Sezgin, *Colloids and Surfaces B: Biointerfaces*, 52 (2006) 1.

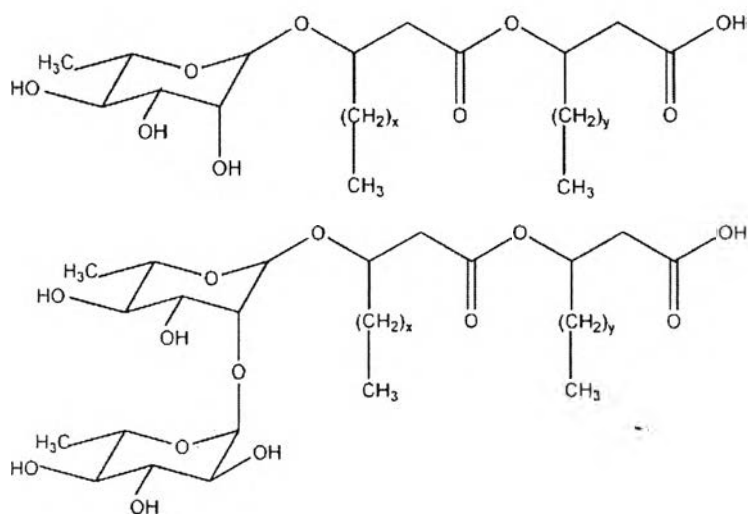


**Figure 5.1** Chemical structures of rhamnolipid biosurfactants.

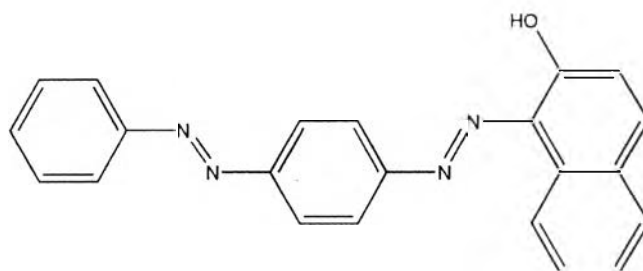


**Figure 5.2** Chemical structure of Sudan III.



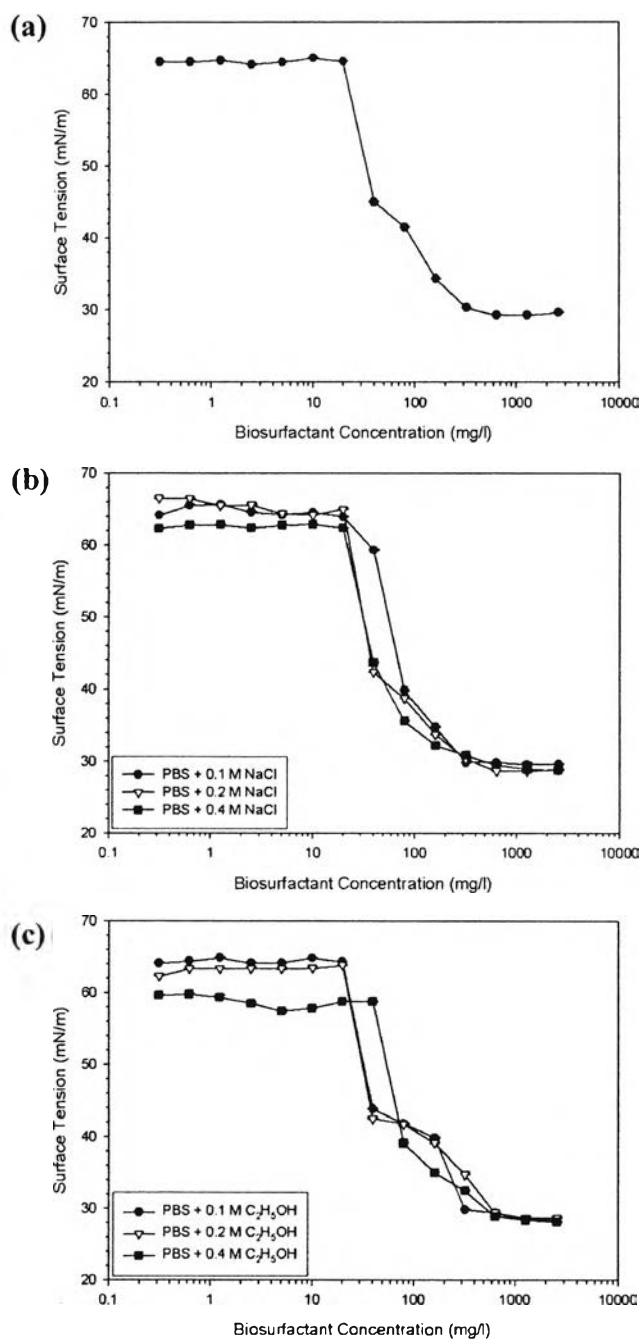


**Figure 5.3** Surface tension *versus* rhamnolipid biosurfactant concentration. (a) PBS solution, (b) PBS solution containing NaCl, and (c) PBS solution containing C<sub>2</sub>H<sub>5</sub>OH.

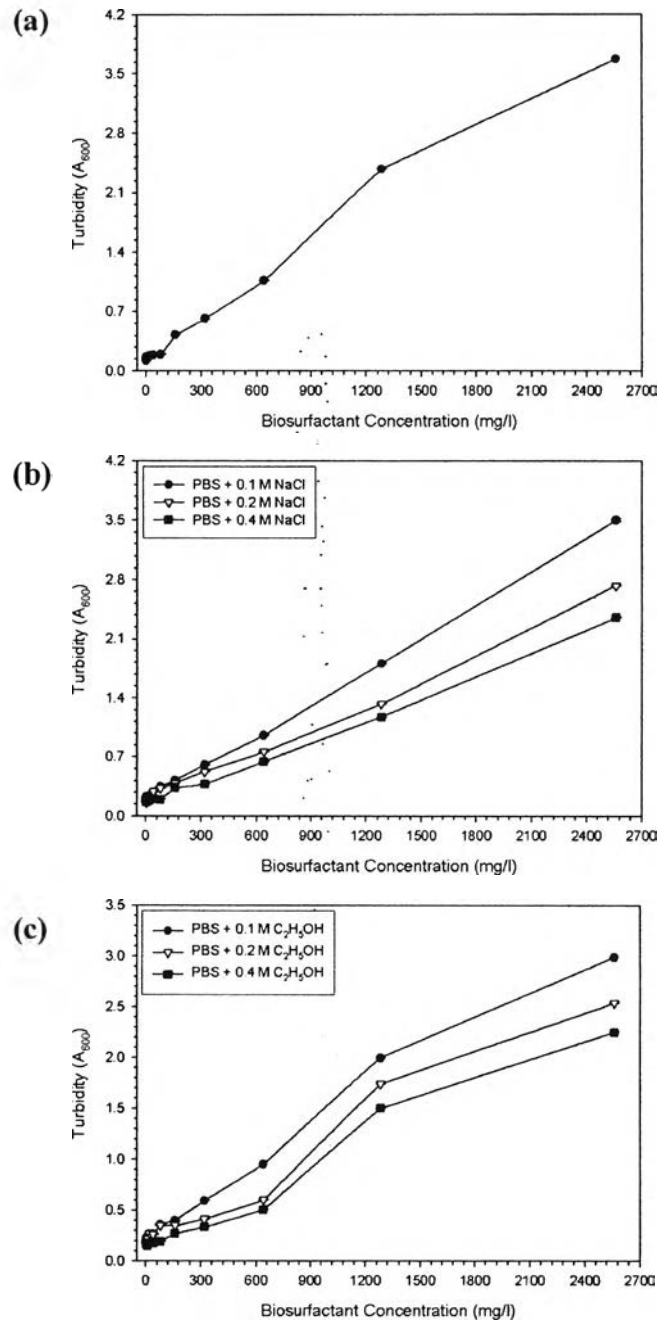


**Figure 5.4** Turbidity (absorbance at 600 nm) of the biosurfactant solution at different concentrations prepared in (a) a PBS solution, (b) a PBS solution containing NaCl, and (c) a PBS solution containing  $C_2H_5OH$ .

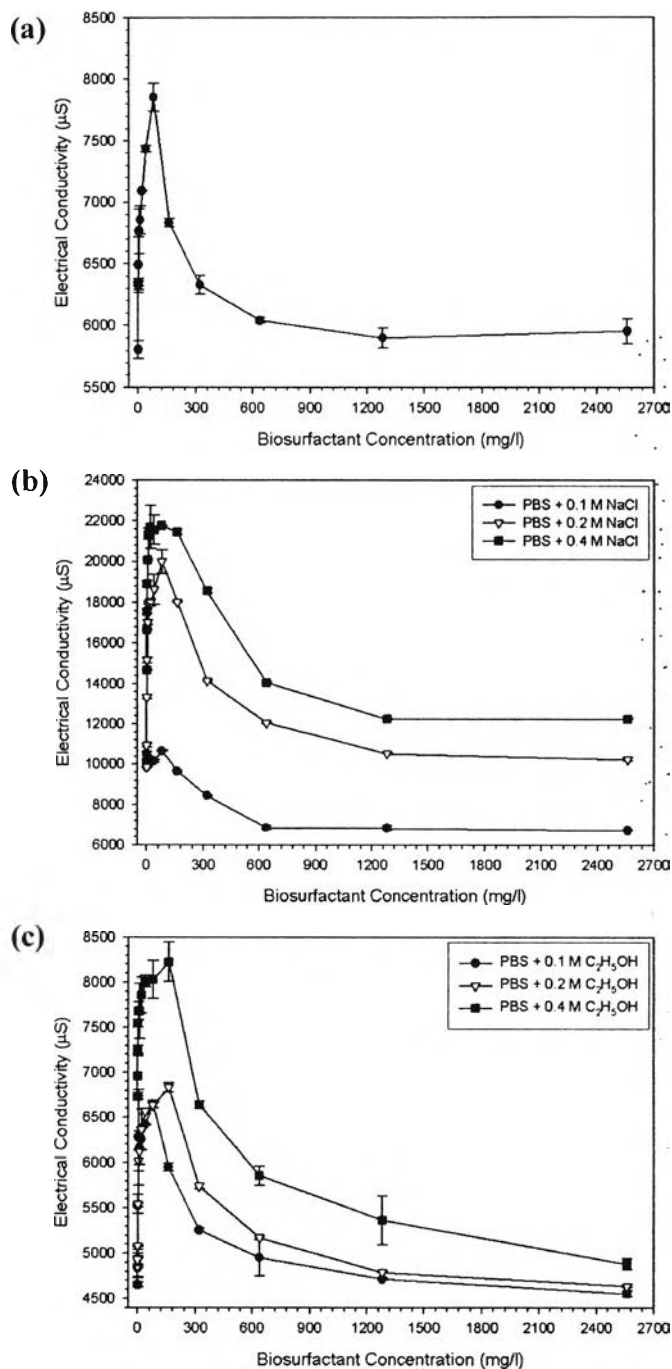


**Figure 5.5** Electrical conductivity of the biosurfactant solution at different concentrations prepared in (a) a PBS solution, (b) a PBS solution containing NaCl, and (c) a PBS solution containing  $\text{C}_2\text{H}_5\text{OH}$ .

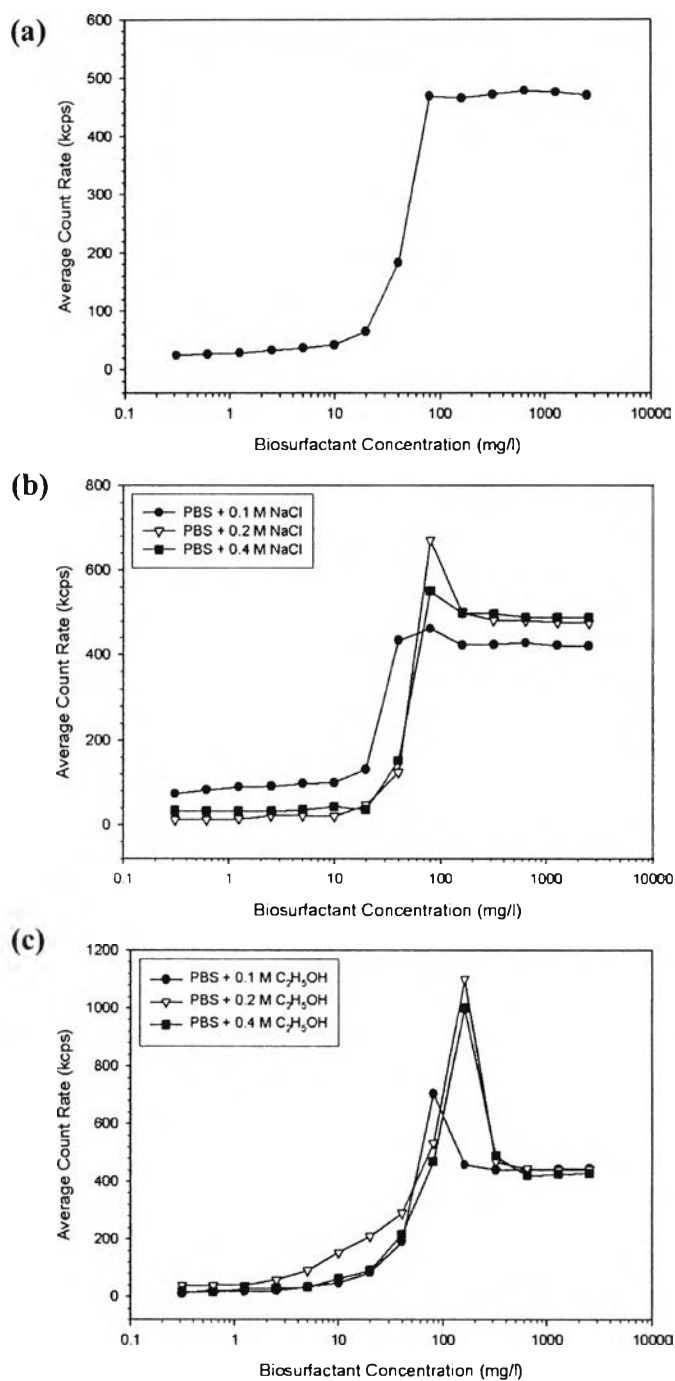


**Figure 5.6** Scattered light intensity of the biosurfactant solution at different concentrations prepared in (a) a PBS solution, (b) a PBS solution containing NaCl, and (c) a PBS solution containing C<sub>2</sub>H<sub>5</sub>OH.

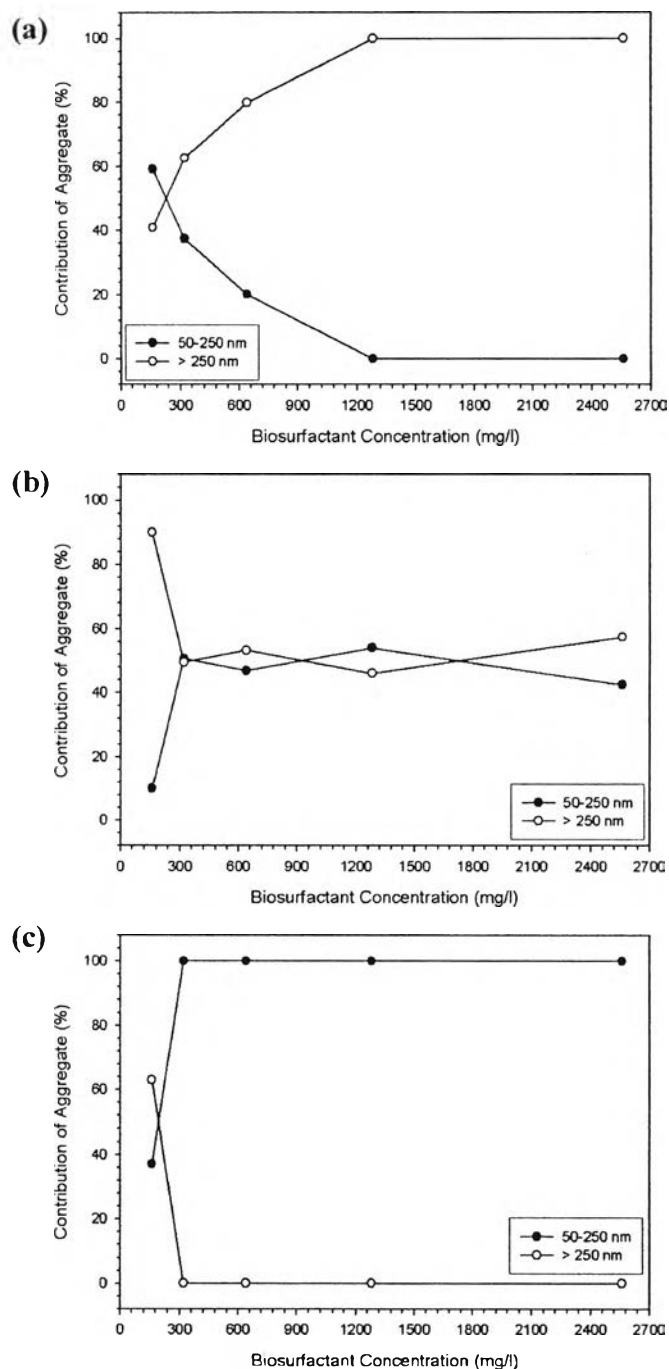


**Figure 5.7** Contribution of the various-sized biosurfactant vesicles at different concentrations prepared in (a) a PBS solution, (b) a PBS solution containing 0.4 M NaCl, and (c) a PBS solution containing 0.4 M C<sub>2</sub>H<sub>5</sub>OH.

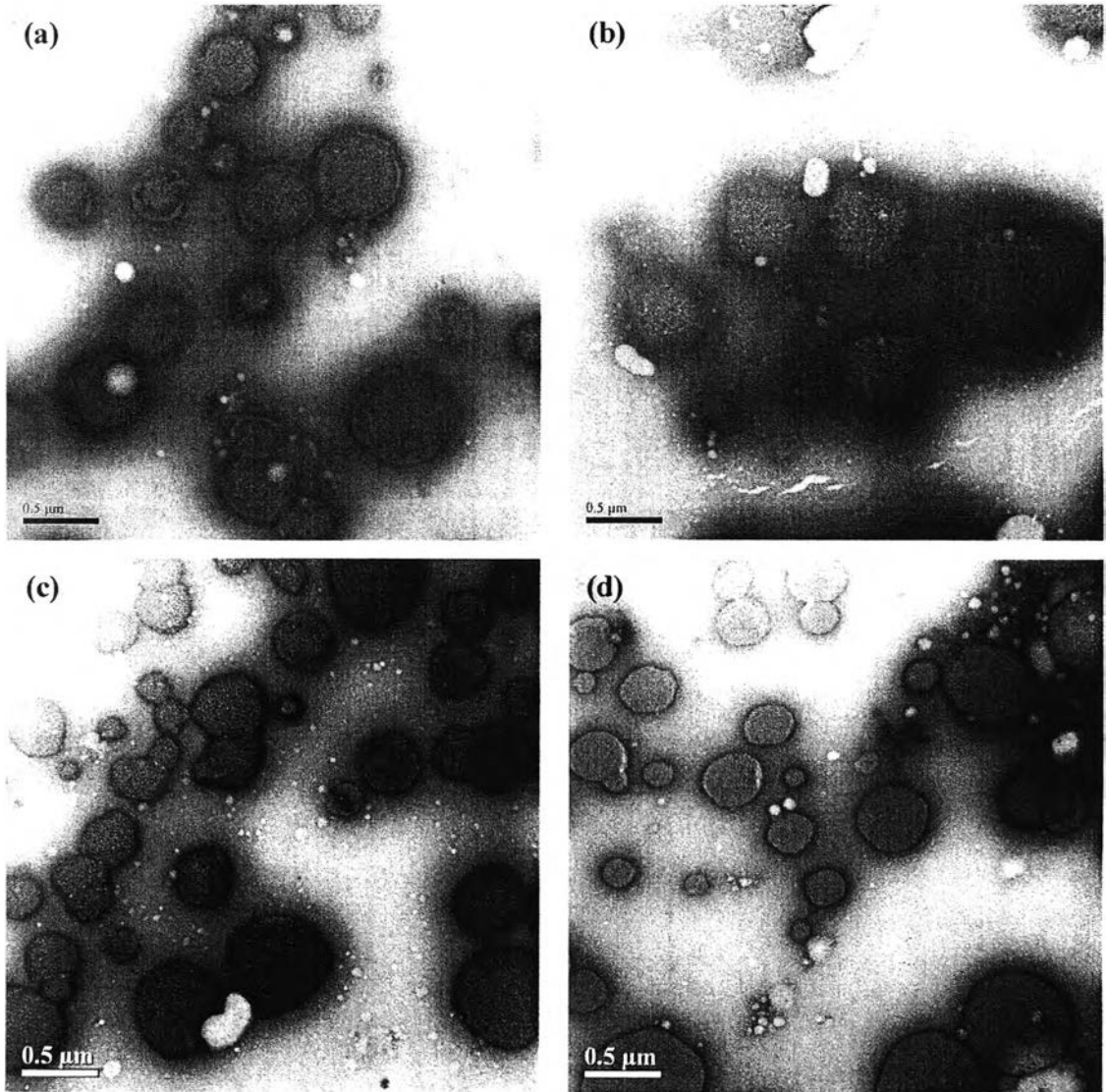


**Figure 5.8** TEM micrographs of the biosurfactant vesicles formed at a concentration of (a) 320 mg/l in a PBS solution and (b) 2560 mg/l in a PBS solution, and (c) a PBS solution containing 0.4 M NaCl, and (d) a PBS solution containing 0.4 M C<sub>2</sub>H<sub>5</sub>OH.

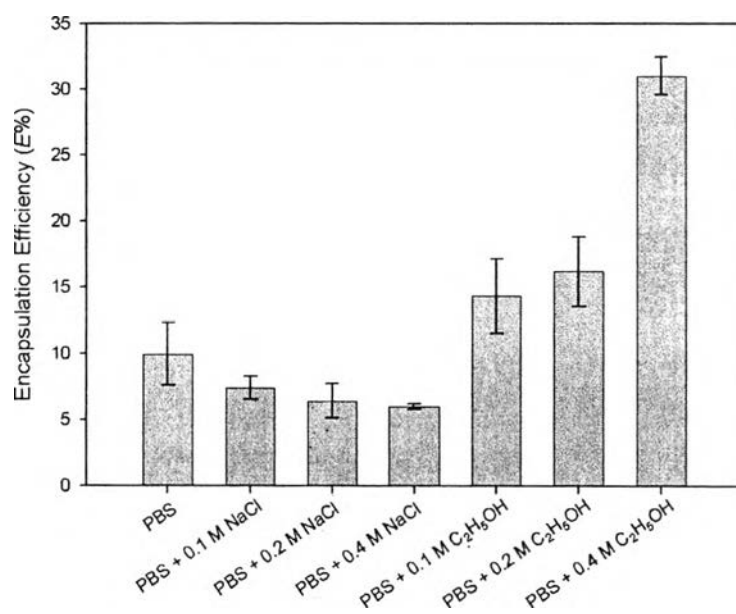


**Figure 5.9** Encapsulation efficiency ( $E\%$ ) of the biosurfactant vesicle formed in a PBS solution in the absence and presence of the additives at a biosurfactant concentration of 1,280 mg/l.